Band structure effects in above threshold photoemission

2011 J. Phys.: Condens. Matter 23 485002

(http://iopscience.iop.org/0953-8984/23/48/485002)

IOP PUBLISHING JOURNAL OF PHYSICS: CONDENSED MATTER

J. Phys.: Condens. Matter **23** (2011) 485002 (5pp) doi:10.1088/0953-8984/23/48/485002

Band structure effects in above threshold photoemission

F Bisio[1], A Winkelmann[2], C-T Chiang[2], H Petek[3] and J Kirschner[2]

[1] CNR-SPIN, Corso Perrone 24, 16152 Genova, Italy
[2] Max-Planck-Institut für Mikrostrukturphysik, Weinberg 2, D-06120 Halle (Saale), Germany
[3] Department of Physics and Astronomy, University of Pittsburgh, PA 15260, USA

E-mail: francesco.bisio@spin.cnr.it

Received 7 September 2011, in final form 11 October 2011
Published 28 October 2011
Online at stacks.iop.org/JPhysCM/23/485002

Abstract

We have performed an angle-resolved two-photon and three-photon photoemission study of the Ag(111) surface employing ultrashort laser pulses as the excitation source. We show the presence of multi-photon resonances between electronic states at selected points of the Brillouin zone which appear in the high-order photoemission spectral region. We observe clear signatures of electronic band structure effects of the Ag crystal in above-threshold photoemission (ATP) processes, identifying two types of transitions, which either proceed via non-resonant multi-photon excitation from an occupied initial state, or involve a real intermediate state located above the vacuum level of the solid directly influencing the ATP process. For this latter class of phenomena, we suggest that electron populations created by incoherent processes give a contribution to the multi-photon transition, possibly allowing us to trace the transmission of photoexcited electrons through the crystal.

(Some figures may appear in colour only in the online journal)

1. Introduction

The nonlinear photoelectric effect induced by ultrashort laser pulses is an extremely powerful tool for investigating the dynamics of electronic excitations at solid surfaces and observing with high resolution the unoccupied band structure of materials [1, 2]. In order not to be overwhelmed by the linear photoemission signal, the photon energy for multi-photon photoemission (mPPE) experiments is usually chosen to be smaller than the vacuum level of the system (E_V), which is in the range of few electronvolts above the Fermi level for most materials. Thus, at the lowest and most easily accessible order of nonlinearity, two-photon photoemission (2PPE), the spectral range of accessible unoccupied electronic states is given by the difference of twice the photon energy and the work function and thus limited by the single photon energy.

Observing the photoemission signal for higher orders of nonlinearity is in principle a practicable way of extending the range of unoccupied electronic states [3]. As well as enabling us to probe more extended energy regions of the band structure, photoemission beyond the second order would also allow the observation of light-induced resonances not accessible to ordinary photoemission or to 2PPE [4, 5], which include the detection of above-threshold photoemission (ATP), i.e. photoemission processes in which electrons absorb more photons than needed to overcome the vacuum barrier [6–11].

Despite this great potential, high-order photoemission from surfaces is a much less-explored field with respect to conventional linear photoemission (PE) or 2PPE. High-order photoemission yields, with few exceptions [11, 5], are indeed low for the typical laser powers employed in surface nonlinear photoemission studies. Augmenting the high-order PE yield by increasing the incident power may lead to the onset of thermionic PE, space charge or other effects that wash out the true electronic band structure effects [12, 13]. However, recent experiments with ultrashort pulse and high repetition rate laser systems have shown that a high peak intensity ($\sim 10^{10}$ W cm^{-2}) can be achieved with nJ/pulse energy [5, 11], paving the way for the observation of band structure features in high-order photoemission.

In this paper we report a 2PPE and three-photon photoemission (3PPE) study of the electronic structure of

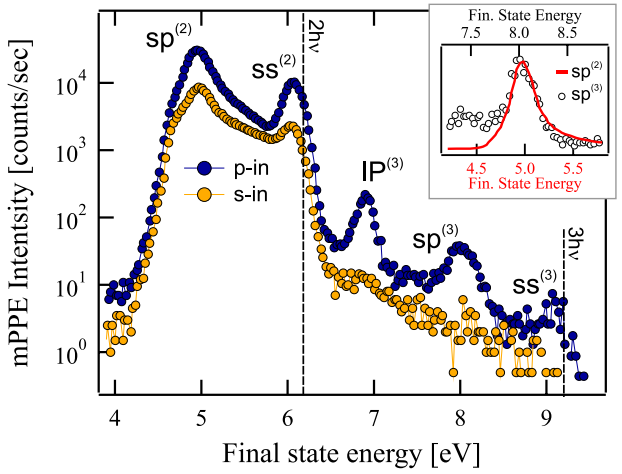

Figure 1. Normal-emission multi-photon spectra from the Ag(111) surface measured with p-polarized and s-polarized radiation (blue and orange markers, respectively). Inset: comparison between the $sp^{(2)}$ and $sp^{(3)}$ peaks (red line and black markers, respectively). Please note that the $sp^{(3)}$ peak in the inset is multiplied by a factor of 850, and that its energy scale (top) is shifted by $h\nu = 3.06$ eV with respect to the $sp^{(2)}$ peak (bottom).

the Ag(111) surface excited by ultrashort laser pulses. We show the presence of multi-photon resonances between electronic states in the high-order PE spectral region, and the clear signature of electronic band structure effects in ATP processes. We distinguish between ATP processes that proceed via non-resonant multi-photon excitation from an occupied initial state and ATP features arising through the resonant coupling of occupied initial states and unoccupied intermediate states located above the vacuum level of Ag(111). The coherent or incoherent contributions to such processes are discussed.

2. Experimental details

2.1. Apparatus

The photoemission experiments were carried out in an ultra-high vacuum system (pressure $< 5\times10^{-11}$ mbar). A self-built Ti:sapphire oscillator provided the frequency-doubled pulses with a central energy of $\hbar\omega = 3.06$ eV, a band width of $\sim$0.17 eV, a pulse length at the surface of $<$18 fs, and a pulse energy of less than 1 nJ. The laser beam was focused on the surface to a spot $\approx$40 μm in diameter. The photoemitted electrons were analyzed by a cylindrical sector analyzer with parallel momentum ($k_\parallel$) resolution below ±0.07 Å^{-1}. The Ag(111) crystal was biased at -1 V. The angle between the incident beam and the axis of the analyzer was fixed at 42°, while the sample could be rotated around an axis normal to the incidence plane to provide a range of electron detection angles with respect to the surface normal of $-35°$ to 35°. A clean and ordered Ag(111) surface was prepared by standard sputtering and annealing procedures. The optical and the electron emission planes were aligned parallel to the [11$\bar{2}$] axis. All the experiments were carried out at 110 K.

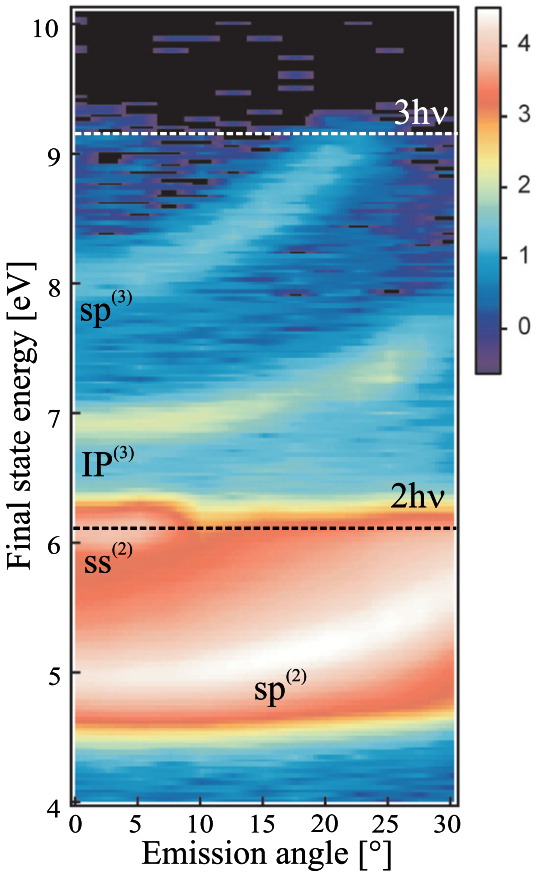

Figure 2. Multi-photon photoelectron intensity (on a logarithmic scale) versus emission angle with respect to the surface normal measured along the [11$\bar{2}$] direction with p-polarized incident radiation.

2.2. Photoemission spectra

In figure 1 we plot the photoelectron yield along the surface normal for p-polarized (p_{in}) and s-polarized (s_{in}) incident radiation (blue and orange markers, respectively), as a function of the final state energy measured with respect to the Fermi level E_F. The 2PPE spectral region extends from the low-energy cutoff to $E = 2h\nu$, while 3PPE spans the $2h\nu < E < 3h\nu$ interval.

Starting from the low-energy side, we observe that the 2PPE region is characterized by two peaks [14, 15], henceforth labeled $sp^{(2)}$ and $ss^{(2)}$, present in both the spectra recorded with nominal p_{in} and s_{in} excitation, with final state energies of $E = 4.94 \pm 0.03$ eV and $E = 6.06 \pm 0.03$ eV, respectively.

In the 3PPE region, the s_{in} spectrum is essentially featureless, while three peaks, labeled $IP^{(3)}$, $sp^{(3)}$ and $ss^{(3)}$, are observed in the p_{in} spectrum at final state energies of 6.89±0.03 eV, 8.00±0.03 eV and 9.12±0.06 eV, respectively.

The p-polarized angle-resolved mPPE spectra from Ag(111) are shown in figure 2. There, we present a color plot of the logarithm of the mPPE yield as a function of the emission angle θ with respect to the surface normal, for p_{in} excitation. In the 2PPE region, a clear upward dispersion of the $sp^{(2)}$ peak is observed, in agreement with

literature data [15]. The $ss^{(2)}$ peak also disperses upwards with increasing θ, crossing the two-photon Fermi level above $\theta = 7.5°$ [16, 15].

In 3PPE, we observe that both $IP^{(3)}$ and $sp^{(3)}$ disperse upwards with increasing θ, while the $ss^{(3)}$ peak becomes quickly undetectable for $\theta > 5°$. Interestingly, we observe that for an emission angle $\theta \approx 25°$, the $IP^{(3)}$ yield which had been steadily decreasing for increasing θ, exhibits a remarkable local increase before dropping off again at larger angles.

In order to summarize the data, we report in figure 3 the energy dispersion curves of the $sp^{(2)}$ (open orange squares), $ss^{(2)}$ (red diamonds), $IP^{(3)}$ (open blue circles) and $sp^{(3)}$ (solid orange squares) peaks as a function of the surface-parallel momentum $k_{\|}$ calculated starting from the data of figure 2. The marker size for the $sp^{(2)}$, $sp^{(3)}$ and $IP^{(3)}$ peaks is proportional to the peak intensity.

3. Discussion

3.1. Resonant coupling in mPPE

The $sp^{(2)}$ peak, based on its energy, emission-angle-dependent intensity and dispersion, can be assigned to the direct transition from the lower (occupied) bulk sp band of Ag(111) and the upper (unoccupied) sp bulk band [17–19, 14, 15]. This electronic transition, observable in 1PPE and 2PPE, represents a prototypical example of bulk-band PE feature. In 2PPE, the $sp^{(2)}$ peak arises due to the coherent two-photon coupling of the lower and upper sp bands, since no real electronic states are available to act as intermediate states in the two-photon process [14].

The $ss^{(2)}$ peak can be reliably ascribed to two-photon photoemission from the well-known occupied L-gap Shockley-type surface state (SS) [20, 16, 21, 22]. The dispersion of the SS can be obtained from the $ss^{(2)}$ curve downshifting it by $2h\nu$ in energy (red line in figure 3).

In the 3PPE region the $IP^{(3)}$ peak can be assigned to the observation of one-photon excitation of electrons from the $n = 1$ image potential (IP) state [23]. In this case, electrons are two-photon excited from an occupied initial state into the IP state and probed by a further photon absorption, thus giving rise to a three-photon process. The IP state dispersion can be obtained downshifting the $IP^{(3)}$ curve by $h\nu$ (solid blue line in figure 3). A fit of the IP state with a parabolic free-electron-like dispersion curve yields an effective mass $m^* = 1.08m_e$ and a binding energy (referred to E_V) of 650 meV. The effective mass is in good agreement with tabulated values, while the binding energy is slightly lower than the established value of (770 ± 30) meV [23–26], possibly because of a slight uncertainty in the exact determination of the vacuum level in our measurements. We notice that, since we observe only the $n = 1$ image potential state, the method by Berthold *et al* for determining the work function based on the extrapolation of the IP Rydberg series [27] is not applicable here.

The calculation of the dispersion curves for the IP and the SS states gives an important clue about the origin of the $IP^{(3)}$ enhancement at $\theta \approx 25°$. For the SS state, the

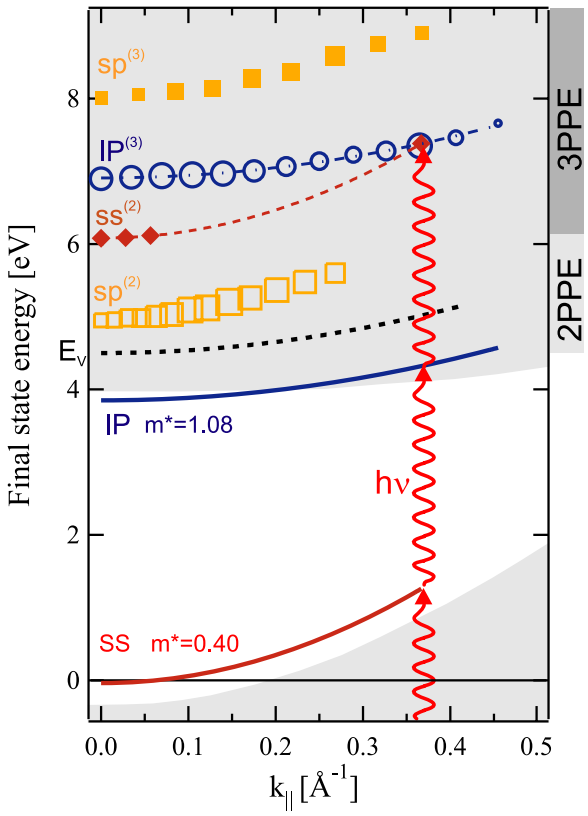

Figure 3. Symbols: experimental final-energy dispersion of the $ss^{(2)}$, $sp^{(2)}$, $sp^{(3)}$ and $IP^{(3)}$ peaks as a function of the surface-parallel momentum along the $[11\bar{2}]$ direction on the Ag(111) surface. The $sp^{(2)}$ and $sp^{(3)}$ peaks are represented by the open and the solid green squares. The $ss^{(2)}$ peak is indicated by solid diamonds. The $IP^{(3)}$ peak is indicated by the open blue circles. The solid blue line represents the electronic dispersion of the IP state, obtained by subtracting one photon energy from the $IP^{(3)}$ peak. The solid red line represents the electronic dispersion of the surface state (SS), obtained subtracting two photon energies from the $ss^{(2)}$ peak. The marker size for $sp^{(2)}$, $sp^{(3)}$ and $IP^{(3)}$ are proportional to the peak intensity.

dispersion calculated from the known values of binding energy and effective mass [16, 22, 28, 29] ($E_{SS}(\bar{\Gamma}) = 63$ meV, $m^* = 0.40m_e$) yields the solid red line in figure 3. At the $k_{\|}$ for which the $IP^{(3)}$ enhancement is observed, we notice that the SS state, dispersing faster than IP, lies exactly one photon energy lower than the IP. The $IP^{(3)}$ enhancement can therefore be ascribed to the resonant coupling of the L-gap Shockley surface state with the $n = 1$ image potential state for parallel momenta away from $\bar{\Gamma}$ which occurs via one-photon excitation of the unoccupied SS followed by another one-photon transition to the IP state and by the further absorption of another ionizing photon that makes this feature observable in 3PPE. The process is pictorially represented in figure 3, with the wavy red lines representing the 'one-photon' coupling. In this context, we show that mPPE can be exploited to achieve light-induced coupling between electronic states not achievable in lower-order photoemission. We incidentally notice that our data about the SS dispersion at $k_{\|} \approx 0.4$ Å^{-1} are consistent with scanning-tunnel spectroscopy (STS) data [22]. However, at

the resolution of the experiments presented here, we cannot exclude deviations from the parabolic dispersion of the Shockley surface state which have recently been demonstrated in mPPE and STS measurements at Cu(111) surfaces [30]. Performing systematic studies with varying incident photon energies would allow us to map the SS dispersion as a function of parallel momentum, exploiting the $k_{\parallel}$-dependent resonance between the SS and IP states. This principle can be readily extended to other electronic states, providing high-resolution band mapping of higher-lying unoccupied states.

3.2. Above-threshold photoemission

The features remaining unassigned in our spectra are the $sp^{(3)}$ and $ss^{(3)}$ peaks. We recall that these two peaks are present (in normal emission) only in the p_{in} spectra while they are not detectable in the s-polarized counterpart. In addition, we notice that these features are both located exactly one photon energy higher than $sp^{(2)}$ and $ss^{(2)}$. For the $sp^{(3)}$ transition, detectable in a broad θ range, this energy shift is constant within the experimental accuracy for all the investigated $k_{\parallel}$ range. Additionally, the peak intensity for $sp^{(3)}$ seems to follow the same pattern as for $sp^{(2)}$, increasing when moving away from normal emission before decreasing again for larger emission angles [15]. A comparison of the shape of $sp^{(2)}$ and $sp^{(3)}$, reported in the inset of figure 1, also shows a remarkable similarity in peak shape: their only clearly discernible difference is a slightly higher low-energy tail for the $sp^{(3)}$ peak. The width of $sp^{(2)}$ is around 200 meV, which only slightly increases to 210 meV for $sp^{(3)}$. In the inset, the energy scale of the 3PPE peak is shifted by $h\nu$ with respect to the 2PPE spectrum, and the $sp^{(3)}$ was multiplied by a factor of 850.

The normal-emission data suggest that the $sp^{(3)}$ and $ss^{(3)}$ peaks arise from a Λ_1-symmetric initial state. Indeed, according to the electric-dipole selection rules for normal emission [31], Λ_1-symmetric initial states are observable in 2PPE under both p_{in} and s_{in} excitation, while their detection is forbidden in 3PPE with s-polarized light.

Altogether, the data suggest that the $sp^{(3)}$ and $ss^{(3)}$ peaks represent the three-photon replicas of the $sp^{(2)}$ and $ss^{(2)}$ peaks. No other electronic states are in fact available within the investigated energy range which could justify the presence of the $sp^{(3)}$ and $ss^{(3)}$ peaks.

Both these 3PPE peaks fall into the broad category of ATP processes, since their two-photon counterparts are already observable in the PE spectra. All electrons with energy $E > E_V + h\nu$ have necessarily undergone ATP processes, but it is important here that we can discern specific band structure features in the ATP part of the photoelectron spectra. The $sp^{(3)}$ and $ss^{(3)}$, though sharing the ATP character, are differently influenced by band structure effects.

For the $ss^{(3)}$ feature, the ATP transition proceeds by a non-resonant multi-photon absorption from the occupied SS at $\bar{\Gamma}$, without involvement of real intermediate states. This type of processes can be seen as related to conventional ATP, dealt with in a relatively large number of works [7, 6, 32, 9, 10, 5], and interpreted based on the theoretical framework for perturbative multi-photon absorption. We merely notice that the $m-$ to $(m+1)$-photon process yield for the SS feature ($ss^{(2)}/ss^{(3)}$ ratio) is of the order of 2×10^3, a value perfectly compatible with those reported under analogous excitation conditions for different surfaces, suggesting a fair generality of the mechanisms involved [6, 10, 5].

More interesting is the case of the $sp^{(3)}$ ATP peak. In this case, the ATP process involves a real penultimate state for the three-photon transition which is located above the $k_{\parallel}$-dependent threshold for electron emission for the whole $k_{\parallel}$ range accessible in our experiment. The observation of the $sp^{(3)}$ peak provides direct access to the electron dynamics in a bulk state, possibly acting as a final state in a photoemission process [17–19, 14, 15], giving additional insights, for example, into the transport of excited valence and core electrons in the band structure, as is currently probed by attosecond experiments [33].

Indirect information about the role of the upper sp band in the $sp^{(3)}$ three-photon process can be inferred from the comparison of the second- and third-order sp peaks (inset of figure 1). Two significant points emerge. Firstly, the presence of a higher low-energy tail in the $sp^{(3)}$ peak compared to $sp^{(2)}$, and secondly the remarkably similar width (210 meV versus 200 meV) of the three-photon and two-photon feature, respectively. Both effects are clearly also observable in spectra measured in off-normal photoemission.

The low-energy tail can be tentatively assigned to electron intraband relaxation in the two-photon excited upper sp band probed by the absorption of a third photon.

The issue of the peak width for the two-photon transition has been thoroughly discussed in [14]. For a two-photon transition measured with a 170 meV laser bandwidth between a continuum of states, as can be naively expected for bulk-band transitions, the expected peak width would be given by the self-convolution of the laser spectrum, plus the broadening given by the photohole and photoelectron relaxation and by the analyzer resolution. Employing the photohole and photoelectron relaxation reported in [14], a peak width for $sp^{(2)}$ of >300 meV would be obtained, which is far too large with respect to the experimental value. The narrowing of the $sp^{(2)}$ peak with respect to such simple expectations was ascribed to the effect of perpendicular momentum conservation on the dipole moment for the sp–sp transition [14], pointing to the limitation of treating bulk-band features as k-independent transitions in a continuum of states [34]. Given the above discussion, it is even more striking to observe a substantially unchanged peak width of the $sp^{(2)}$ and the $sp^{(3)}$ feature. Indeed, the three-photon process giving rise to $sp^{(3)}$ involves additional broadening mechanisms with respect to its 2PPE counterpart, arising from the additional action of the laser bandwidth on the two-photon peak and from the presence of a further intermediate state in the transition. A reliable fully quantitative model of the four-level system [4] requires *a priori* information on the relaxation dynamics in all the intermediate states, and is thus far beyond the scope of this work. From a qualitative point of view, however, the observation of comparable width of the $sp^{(3)}$ and $sp^{(2)}$ peaks clearly points to the existence in the

three-photon process of an efficient mechanism of bandwidth narrowing. We suggest that such a mechanism is related to the possible presence of significant coherent contributions to the excitation pathway for the 3PPE peak, that effectively provide an energy filtering mechanism as discussed in more depth in [4].

Time-domain experiments on the $sp^{(2)}$ and $sp^{(3)}$ peaks might help elucidate the relative weight of coherent and incoherent excitation pathways in the ATP three-photon process, allowing us to assess the possible buildup of the electronic population in the upper sp band and quantify the relaxation rate of the photoelectrons in the upper sp band, with important implications for the understanding of electron dynamics in PE phenomena.

4. Conclusion

We have performed an angle-resolved multi-photon photoemission study of the Ag(111) surface employing ultrashort laser pulses as the excitation source. We have shown the presence of resonances in the spectra ascribed to multi-photon transitions between occupied and unoccupied electronic states on the surface at a specific point of the Brillouin zone, and the fingerprint of band structure features in above-threshold photoemission processes. We distinguished between above-threshold transitions that proceed via non-resonant multi-photon excitation from an occupied initial state and ATP transitions involving an intermediate state located above the vacuum level of Ag(111). In the second category, we observed an ATP peak arising from a multi-photon transition between occupied and unoccupied bulk sp bands. The presence of an incoherent contribution to this transition suggested the possibility of directly observing an electronic population in a state above the vacuum level of a solid.

In perspective, observing the dynamics of such ATP transitions in the time domain could yield valuable information about the relaxation process in the unoccupied sp band.

Acknowledgments

F B acknowledges support from the MIUR (project no. PRIN 2008AKZSXY_002). HP acknowledges financial support from NSF grant CHE-0911456.

References

[1] Petek H and Ogawa S 1997 *Prog. Surf. Sci.* **55** 239
[2] Fauster T, Weinelt M and Höfer U 2007 *Prog. Surf. Sci.* **82** 224
[3] Bovensiepen U, Petek H and Wolf M (ed) 2010 *Dynamics at Solid State Surfaces and Interfaces* (*Current Developments*) vol 1 (Weinheim, Germany: Wiley–VCH) chapter 2
[4] Winkelmann A, Lin W-C, Chiang C-T, Bisio F, Petek H and Kirschner J 2009 *Phys. Rev.* B **80** 155128
[5] Bisio F, Nývlt M, Franta J, Petek H and Kirschner J 2006 *Phys. Rev. Lett.* **96** 087601
[6] Fann W S, Storz R and Bokor J 1991 *Phys. Rev.* B **44** R10980
[7] Farkas Gy and Tóth Cs 1990 *Phys. Rev.* A **41** R4123
[8] Farkas Gy, Tóth Cs, Moustaizis S D, Papadogiannis N A and Fotakis C 1992 *Phys. Rev.* A **46** R3605
[9] Georges A T 2002 *Phys. Rev.* A **66** 063412
[10] Banfi F, Giannetti C, Ferrini G, Galimberti G, Pagliara S and Parmigiani F 2005 *Phys. Rev. Lett.* **94** 037601
[11] Schenk M, Krüger M and Hommelhoff P 2010 *Phys. Rev. Lett.* **105** 257601
[12] Fujimoto J G, Liu J M, Ippen E P and Bloembergen N 1984 *Phys. Rev. Lett.* **53** 1837
[13] Aeschlimann M, Schmuttenmaer C A, Elsayed-Ali H E, Miller R D J, Cao J, Gao Y and Mantell D A 1995 *J. Chem. Phys.* **102** 8606
[14] Pontius N, Sametoglu V and Petek H 2005 *Phys. Rev.* B **72** 115105
[15] Winkelmann A, Sametoglu V, Zhao J, Kubo A and Petek H 2007 *Phys. Rev.* B **76** 195428
[16] Paniago R, Matzdorf R, Meister G and Goldmann A 1995 *Surf. Sci.* **336** 113
[17] Nelson J G, Kim S, Gignac W J, Williams R S, Tobin J G, Robey S W and Shirley D A 1985 *Phys. Rev.* B **32** 3465
[18] Miller T, McMahon W E and Chiang T-C 1996 *Phys. Rev. Lett.* **77** 1167
[19] Miller T, Hansen E D, McMahon W E and Chiang T-C 1997 *Surf. Sci.* **376** 32
[20] Heimann P, Neddermeyer H and Roloff H F 1977 *J. Phys. C: Solid State Phys.* **10** L17
[21] Nicolay G, Reinert F, Schmidt S, Ehm D, Steiner P and Hüfner S 2000 *Phys. Rev.* B **62** 1631
[22] Bürgi L, Petersen L, Brune H and Kern K 2000 *Surf. Sci.* **447** L157
[23] Giesen K, Hage F, Himpsel F J, Riess H J, Steinmann W and Smith N V 1987 *Phys. Rev.* B **35** 975
[24] Giesen K, Hage F, Himpsel F J, Riess H J and Steinmann W 1985 *Phys. Rev. Lett.* **55** 300
[25] Lingle R L, Padowitz D F, Jordan R E, McNeill J D and Harris C B 1994 *Phys. Rev. Lett.* **72** 2243
[26] Lingle R L Jr, Ge N-H, Jordan R E, McNeill J D and Harris C B 1996 *Chem. Phys.* **205** 191
[27] Berthold W, Rebentrost F, Feulner P and Höfer U 2004 *Appl. Phys.* A **78** 131
[28] Reinert F, Nicolay G, Schmidt S, Ehm D and Hüfner S 2001 *Phys. Rev.* B **63** 115415
[29] Kliewer J, Berndt R, Chulkov E V, Silkin V M, Echenique P M and Crampin S 2000 *Science* **288** 1399
[30] Ünal A A, Tusche C, Ouazi S, Wedekind S, Chiang C-T, Winkelmann A, Sander D, Henk J and Kirschner J 2011 *Phys. Rev.* B **84** 073107
[31] Hermanson J 1977 *Solid State Commun.* **22** 9
[32] Mishra A and Gersten J I 1991 *Phys. Rev.* B **43** 1883
[33] Cavalieri A L *et al* 2007 *Nature* **449** 1029
[34] Hansen E D, Miller T and Chiang T C 1998 *Phys. Rev. Lett.* **80** 1766